Rigorous Kinetic Models for Catalyst Deactivation by Coke Deposition: Application to Butene Dehydrogenation[1]

G. B. MARIN, J. W. BEECKMAN,[2] AND G. F. FROMENT

Laboratorium voor Petrochemische Techniek, Rijksuniversiteit Gent, Krijgslaan 281, B-9000 Gent, Belgium

Recently developed models describing catalyst deactivation in terms of coverage of active sites and blockage of pores are extended and applied to published data on the dehydrogenation of butene on a chromia–alumina catalyst. The textural and catalytic properties of the catalyst are determined by classical physicochemical techniques. Regression of the coke versus time-on-stream curves allows the estimation of fundamental properties of the coke such as molecular mass and enables an insight into the mechanism of coke formation to be obtained. The best regression results are obtained by considering two stages in the coke formation sequence: there is a first stage of site coverage by coke precursor accompanied by instantaneous growth up to an intermediate size and a second stage of further growth at a rate of the same order of magnitude as the rate of coke formation corresponding to the first stage. Some 15% of the catalyst surface becomes inaccessible by blockage of the smallest pores. The deactivation of the dehydrogenation itself is predicted in a satisfactory way by using the parameter estimates derived from the coking data only. © 1986 Academic Press, Inc.

INTRODUCTION

Many petrochemical and petroleum refining processes are accompanied by side reactions leading to carbonaceous material, called coke, which affects the catalyst activity and selectivity. Frequently, the original activity and selectivity can be restored by controlled combustion. The implications can be far-reaching: in the catalytic cracking of gas oil and the catalytic reforming of naphtha, fluidized-bed and moving-bed technology were introduced to allow continuous regeneration. A theoretical framework linking the deactivation to the chemical and textural properties of the catalyst is required as a basis for the quantitative description of the phenomena involved.

Recently, Beeckman and Froment (*1–3*) provided a quantitative analysis of the deactivation of amorphous catalysts by coke deposition in terms of active site coverage and pore blockage. In their approach, the catalyst texture is represented by a network of pores structured as a tree, with a degree of branching equal to 2 (*4–6*). The bonds of the tree correspond to the pores of the catalyst, the nodes to their intersection. Each pore is characterized by two stochastic variables: the pore length, L, and the pore diameter, D. The probability density function of the former, $\lambda(L)$, is derived from the assumption that the branching probability, νdL, is independent of the pore length and, hence, is of the Poisson type

$$\lambda(L) = \nu e^{-\nu L} \tag{1}$$

with ν^{-1} the average pore length. The probability density function of the pore diameter, $g^S(D)$, can be obtained from nitrogen desorption and mercury penetration curves. The deactivation of the catalyst is accounted for by multiplying the initial reaction rate, $r°$, with a deactivation function, ϕ, the average probability that a randomly taken site of the pore network is active, i.e., not covered and still accessible. Consequently, ϕ equals the product of the prob-

ability for the sites to be accessible, P, with the conditional probability, S, that the accessible site is not covered:

$$\frac{r}{r^\circ} = \phi = PS. \qquad (2)$$

Beeckman and Froment (1, 2) arrived at expressions for ϕ as a function of observable properties by making the following assumptions:

(i) both the main and the coking reaction occur on one and the same single site of the catalyst;

(ii) coverage of the sites by coke occurs in a random way;

(iii) there are no concentration gradients of reactants or reaction products inside the catalyst pellet.

The second factor in the right-hand side of Eq. (2) is then given by (1)

$$S = \exp(-R_s^\circ t) \qquad (3)$$

with

$$R_s^\circ = \sum_i r_{s,i}^\circ \qquad (4)$$

and

$$r_{s,i}^\circ = f_i(p_A, p_B, T, \ldots ; k_C, K_A, \ldots). \qquad (5)$$

The rate of fractional site coverage, $r_{s,i}^\circ$, corresponds to a reaction path from a gas phase component i leading to coke and depends upon the process conditions only.

Several expressions were derived for the accessibility function, P, corresponding to specific assumptions about the network of pores and the coke formation. They contain two groups of fundamental parameters. The first group is related to the textural properties of the catalyst, such as the distribution of pore diameters, the specific catalyst surface area, A_S, and the average pore length. The second group relates to the cause of the deactivation, the formation of coke. It consists of the physical properties of the coke, such as molecular mass, M, and density, ρ,

and of the parameters involved in the rate expressions for coke formation. As the amount of coke increases, the accessibility decreases and therefore time enters into the expressions for P.

Deactivation results from irreversible adsorption on active sites. The coke precursor is considered to be the first irreversibly adsorbed component in a sequence of steps leading to coke. In a first paper Beeckman and Froment (1) assumed that the formation of the coke precursor was the rate-determining step in the coke formation. In other words, the growth of the coke following upon the precursor formation was considered to be instantaneous. In a second paper the initial rate of coke accumulation due to growth, r_p°, was considered to be of the same order of magnitude as the initial rate of site coverage (2). The rate of growth depends only upon the process conditions:

$$r_p^\circ = h(p_A, p_B, T,$$
$$\ldots ; k_C', K_A, \ldots). \qquad (6)$$

Both approaches lead to equations yielding the coke content of the catalyst, C_C, as a function of time. The parameters in these equations are identical to those occurring in the expressions for the accessibility and the deactivation functions.

Combining the equations for the coke content with Eq. (2) yields the following general expression for the deactivation function of a reaction:

$$\phi = \phi(C_C; g^S(D), A_S, \nu,$$
$$C_t, M_C, \rho, R_s^\circ, r_p^\circ). \qquad (7)$$

The expression (7) derived from this approach differs from the simple but empirical time-dependent expressions for deactivation functions used so far by several authors (7–13) in that they contain parameters rigorously related to the cause of the deactivation.

The present paper is intended to illustrate the application of the rigorous approach defined above to an industrial process, namely, the dehydrogenation of butene to

butadiene over a 20 wt% Cr_2O_3 on Al_2O_3 catalyst.

METHODS AND THEORETICAL ANALYSIS

1. Characterization of the Catalyst Texture

Electron microscopy showed that the chromia–alumina catalyst contains aggregated primary particles. The aggregates have an average diameter of 5×10^3 nm. The primary particles are formed by the Al_2O_3 support. The voids in the aggregates consist of mesopores, i.e., pores with a diameter between 2 and 50 nm. The dimensions of the voids around the aggregates fall in the macropore region. The pore-diameter distribution of the catalyst has been reported by Beeckman and Froment (1). The macropores account for 42% of the void space and 2% of the surface area. The other fraction consists of mesopores. Assuming a cylindrical shape for the pores, a specific surface area of 65 m²/g cat was derived from the pore-diameter distribution. This is in good agreement with the BET surface area of 67 m²/g cat.

In the present work the catalyst texture is described by the combination of the properties of a tree and of a simplified Wheeler (14) model, i.e., consisting of cylindrical non-interconnecting mesopores, with an average length of 5×10^3 nm, surrounded by macropores. This type of network corresponds to the so-called micro–macro network considered by Beeckman and Froment (1, 2). The distribution in diameter of the mesopores is accounted for.

2. Kinetics of Coke Deposition

A comprehensive experimental study of the coke formation accompanying the dehydrogenation of butene on the catalyst described in Section 1 above was carried out by Dumez and Froment (15). The catalyst particle diameter was limited to 0.7 mm to avoid internal concentration gradients. Coke content versus time curves were obtained over a wide range of temperatures and feed compositions by means of a dif-

ferentially operated electrobalance. Coke deposition originated from both butene and butadiene, while hydrogen exerted an inhibiting effect. The coke on the catalyst was shown to deactivate its own formation. The relation (7) between the deactivation function and the coke content was identical for coke deposition from butene or butadiene and almost independent of the process conditions. This suggests that the molecular mass and the density of the coke originating from butene are identical to those of the coke originating from butadiene and do not depend strongly on the process conditions. For a single site mechanism the classical Hougen–Watson approach leads to the following equation for the initial total rate of fractional site coverage:

$$R_s^\circ = \frac{A_A^\circ \exp(-E_A/RT)p_A + A_D^\circ \exp(-E_D/RT)p_D}{1 + K_A p_A + K_D p_D + K_H p_H}.$$

$$(8)$$

In this equation the concentrations of adsorbed intermediates between butene and butadiene and the corresponding coke precursors are neglected.

2.1. Instantaneous growth of coke. In this situation coke reaches its ultimate size within an infinitely small time interval following upon the coke precursor formation. The molecular mass of the coke, M_C, is unique and independent of time.

Extending the expression for the coke content of a micro–macro network derived by Beeckman and Froment (1) by taking into account the distribution of the pore diameter leads to

$$\hat{C}_C(D,t) = C_t \frac{\nu}{\sigma(D)} \rho V(D)$$

$$\left\{ 2 \ln \left(1 + \frac{\sigma(D)}{\nu} (1 - \exp(-R_s^\circ t)) \right) \right.$$

$$\left. + 1 \middle/ \left(1 + \frac{\sigma(D)}{\nu} (1 - \exp(-R_s^\circ t)) \right) - 1 \right\}$$

$$(9)$$

for the average coke content in the pores which can be blocked, and to

TABLE 1

Instantaneous Coke Growth: Results of Regression
of the Complete Set of Coking Curves with Model
Equations (8)–(14)[a]

Parameter	Value	t value
M_C (kg coke/kmol coke)	1.892×10^4	71.5
A_A° (1/bar · h)	6.855×10^8	15.2[b]
E_A (kJ/kmol)	1.256×10^5	30.2
A_D° (1/bar · h)	3.980×10^6	21.8[b]
E_D (kJ/kmol)	8.105×10^4	30.0
K_A (1/bar)	2.801	4.6
K_D (1/bar)	7.785	6.1
K_H (1/bar)	18.61	15.1
F value	4408	

[a] $\rho = 1.8 \times 10^3$ kg coke/kg cat; $C_t = 3.8 \times 10^{-6}$ kmol
sites/kg cat; $\nu^{-1} = 5 \times 10^3$ nm.

[b] On the reparametrized preexponential factors.

$$C_C(D > D_C, t) = (1 - \gamma)C_t M_C(1 - \exp(-R_s^\circ t)) \quad (10)$$

for the coke content in the pores which cannot be blocked, with

$$D_C = \left(\frac{6M_C}{\pi \rho N_A}\right)^{1/3} \quad (11)$$

$$V(D) = \frac{\pi D^3 N_A}{6} \quad (12)$$

$$\sigma(D) = \frac{\pi D C_t N_A}{A_S}. \quad (13)$$

The total coke content of the catalyst follows from

$$C_C(t) = \int_0^{D_C} g^S(D)\hat{C}_C(D,t)dD + C_C(D > D_C, t). \quad (14)$$

The coke diameter, D_C, is derived from the molecular mass by assuming a spherical shape of the coke molecule. In the fraction, γ, of pores with a diameter smaller than D_C, the coke diameter equals the pore diameter.

Values for the textural parameters of the catalyst are obtained from the independent physical measurements mentioned in the preceding paragraph. A density of 1800 kg/m³ was assigned to the deposited coke (16,

17). A value of 3.8×10^{-6} kmol sites/kg cat based on O_2 uptake data (18, 19) was assigned to the total concentration of active sites.

The number of parameters in Eqs. (8)–(14) amounts to 8. Their value has to be determined from the observations of the coke deposition kinetics. This was done by a nonlinear regression of the complete set of data, i.e., covering a wide range of temperatures and feed compositions, using the Marquardt algorithm. The regression was performed after the reparametrization of the preexponential factors according to

$$A^\circ = A^{\circ\prime} \exp(E/RT_m) \quad (15)$$

with T_m the average temperature of the experimental data. Table 1 lists the estimates for the parameters with their corresponding approximate individual t values. The significance of the global regression is expressed by the ratio of the mean regression sum of squares to the mean residual sum of squares, F (20). The F value is high, indicating an excellent fit, while the t values associated with the parameters lead to significant estimates for the latter. The highest binary correlation coefficient between the parameter estimates amounts to 0.44. Figure 1 compares experimental and calculated coke contents for a typical set of reaction conditions.

The coke diameter derived from Eq. (11) and the molecular mass listed in Table 1 amounts to 3.22 nm. This is sufficiently large to render 13.1% of the catalyst surface area inaccessible by pore blockage. The average site density in the pores which can be blocked equals 2.81×10^8 m⁻¹ and corresponds to 1.41×10^3 active sites per pore. Because of this high number of active sites per pore and the absence of connectivity between the mesopores, blockage occurs within a few seconds. Hence, little coke is deposited in these pores, as shown in Fig. 1. At infinite time a value for the coke content of 5.10×10^{-6} kg coke/kg cat is obtained from the first term in Eq. (14). This value can be neglected with respect to the
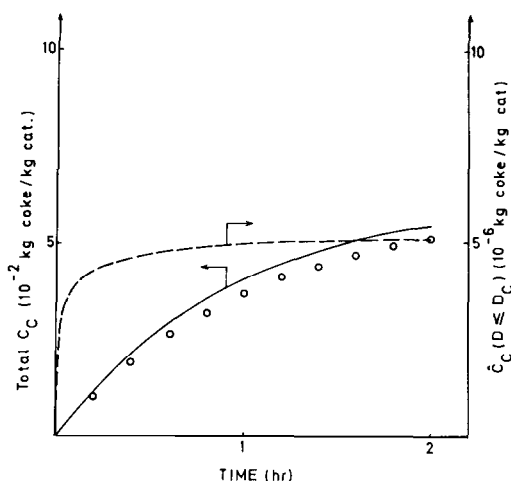
FIG. 1. Coke content versus time at 823 K, p_A = 0.240 bar, $p_B = p_H$ = 0.0 bar. Experimental points from Ref. (15). Solid line: total coke content calculated with instantaneous growth equations. Dashed line: coke content in pores which can be blocked calculated with Eq. (9). Parameter values from Table 1.

value of 6.26×10^{-2} kg coke/kg cat at infinite time for the coke content in the pores which cannot be blocked. The contributions to the coke content by the two terms in Eq. (14) are comparable during the first seconds of the deactivation only. A significant separate determination of C_t and M_C can only be expected from kinetic data collected during this initial time period since the second term of Eq. (14) contains the product $C_t M_C$, whereas the first term is proportional to C_t alone.

Finally, it should be noted that expressions for the rate of fractional site coverage other than those leading to (8) were tested. This led to only marginal changes of the significance of the global regression.

2.2. *Instantaneous growth followed by growth at a finite rate.* The model described in Section 2.1 assumes that the rate constants of all the elementary steps following the coke precursor formation are much larger than the rate constant of the formation of the coke precursor itself. In their second paper Beeckman and Froment (2) no longer assumed the rate constants of further growth to be much larger than the rate

constant of the formation of coke precursor. This led to a finite rate of growth which was considered to be independent of the size of the coke. Another possibility would be that the rate constants of growth decrease with the size of the coke. The model developed next may be considered as an extension of the second model proposed by Beeckman and Froment (2). Indeed, the latter comprises two stages, one of coke precursor formation and one of further growth at a finite rate, r_p^o. If the first stage is not limited to coke precursor formation, but extends to coke with a molecular mass, M_{CI}, corresponding to a size intermediate between that of the coke precursor and of the ultimate coke molecule, an approximation of the decrease of rate constants of the growth steps is obtained. In this situation coke reaches a unique intermediate size within an infinitely small time interval following upon the formation of a coke precursor. The rate of coke formation corresponding to this first stage is controlled by the coke precursor formation, i.e., the rate of fractional site coverage.

Blockage of pores can occur immediately after site coverage when the diameter of the coke, D_{CI}, corresponding to M_{CI} is sufficiently large to cause blockage. The average coke content in such pores is obtained from an expression analogous to Eq. (9) with $D \leq D_{CI}$.

In pores in which further growth at a finite rate can occur, the volume of a typical coke molecule, V_C^*, is obtained by integration of

$$\frac{dV_C^*}{d(t - t^*)} = \frac{r_p^o}{\rho N_A C_t} \qquad (16)$$

$$V_{CI}^* = \frac{M_{CI}}{\rho N_A} \qquad \text{at } t = t^* \quad (17)$$

with t^* the time at which the corresponding site has been covered. If r_p^o does not depend on V_C^* or time, a linear relation with time is obtained for given process conditions:

$$V_C^* = \frac{M_{CI}}{\rho N_A} + \frac{r_p^o}{\rho N_A C_t} (t - t^*). \quad (18)$$

TABLE 2

Instantaneous Growth Followed by Growth at a Finite Rate: Results of Regression of the Complete Set of Coking Curves with Model Equations (8), (9), (12), (13), and (20)–(22)[a]

Parameter	Value	t value
$\dfrac{r_p^\circ}{R_s^\circ}$ (kg coke/kg cat)	3.775×10^{-3}	20.6
M_{CI} (kg coke/kmol coke)	1.196×10^4	39.6
A_A° (1/bar · h)	4.908×10^9	15.0^b
E_A (kJ/kmol)	1.353×10^5	39.1
A_D° (1/bar · h)	2.096×10^7	19.2^b
E_D (kJ/kmol)	8.887×10^4	36.3
K_A (1/bar)	2.086	4.8
K_D (1/bar)	3.250	3.9
K_H (1/bar)	20.60	17.8
F value	5981	

[a] $\rho = 1.8 \times 10^3$ kg coke/kg cat; $C_t = 3.8 \times 10^{-6}$ kmol sites/kg cat; $\nu^{-1} = 5 \times 10^3$ nm.

[b] On the reparametrized preexponential factors.

The corresponding molecular mass is given by

$$M_C^* = M_{CI} + \frac{r_p^\circ}{C_t}(t - t^*). \qquad (19)$$

The time required to block a pore with diameter D is then given by

$$t_b(D) = \frac{C_t}{r_p^\circ}(\rho V(D) - M_{CI}). \qquad (20)$$

The coke content in the pores too large to be blocked is obtained from

$$\hat{C}_C(D,t) = C_t M_{CI}(1 - \exp(-R_s^\circ t))$$

$$+ r_p^\circ \left(t - \frac{1}{R_s^\circ}(1 - \exp(-R_s^\circ t)) \right). \qquad (21)$$

The first term in Eq. (21) represents the coke content corresponding to the molecular mass M_{CI}. The second term accounts for the coke growth at a finite rate from coke with molecular mass M_{CI} onward.

Pores with an intermediate diameter can be blocked by growth of the coke at a finite rate. The corresponding coke content is given by Eq. (21) before blockage can occur and by Eq. (82) of Ref. (2) where the molecular mass of coke precursor should be re-

placed by the intermediate molecular mass, M_{CI}, after blockage can occur.

Integration over the pore-diameter distribution yields the total coke content:

$$C_C(t) = \int_0^\infty g^S(D)\hat{C}_C(D,t)\, dD. \qquad (22)$$

When the ratio of the finite rate of growth to the rate of fractional site coverage, r_p°/R_s°, is independent of the process conditions, the model equations (8), (9), (12), (13), and (20)–(22) contain one additional parameter in comparison to the model equations (8)–(14) for single-stage coke formation. Table 2 shows the regression results obtained with the equations for two-stage coke formation. The ratio of r_p° to R_s° is significantly different from zero at a probability level higher than 99.9%. The global regression of the data, as expressed by the F value, is superior to that obtained by the single-stage instantaneous growth model. The highest binary correlation coefficient between the parameter estimates amounts to 0.76. The improved regression of the experimental data is illustrated by Fig. 2.
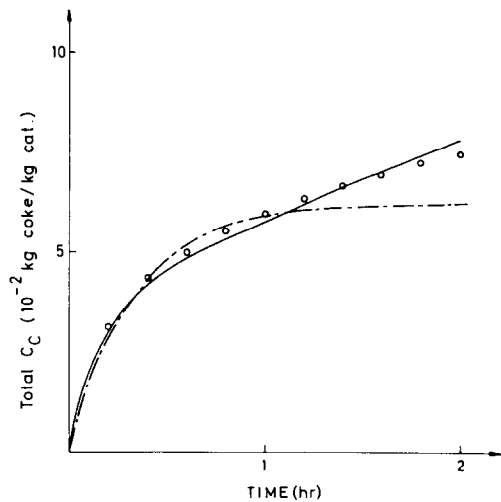
Again, as in the case of single-stage in-

FIG. 2. Coke content versus time at 873 K. $p_A = 0.238$ bar, $p_B = p_H = 0.0$ bar. Experimental points from Ref. (15). Solid line: calculated with equations corresponding to instantaneous growth followed by growth at a finite rate and parameter values from Table 2. Dashed line: calculated with instantaneous growth equations and parameter values from Table 1.
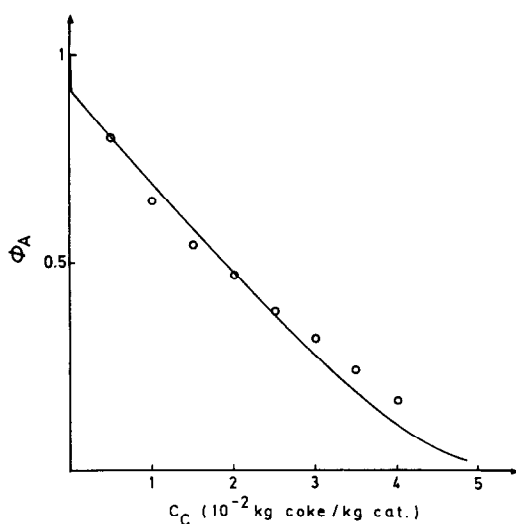
FIG. 3. Deactivation function for dehydrogenation versus coke content at 843 K, $p_A = 0.0369$ bar, $p_B = p_H = 0.0$ bar. Experimental points from Ref. (15). Solid line: calculated with Eqs. (22) and (27) and parameter values from Table 2.

stantaneous growth, the coke content in the pores which can be blocked is negligible with respect to the total coke content. The coke content of the catalyst is essentially calculated by Eq. (21) and depends only on the product $C_t M_{CI}$, not on C_t and M_{CI} separately. Hence, the estimate for M_{CI} is inversely proportional to the value assigned to the total concentration of active sites. The instantaneously reached molecular mass of the coke reported in Table 2 corresponds to a sphere with a diameter of 2.76 nm. This size is sufficiently large to render 9.6% of the catalyst surface area inaccessible by blockage of the smallest pores.

The estimate for the r_p°/R_s° ratio listed in Table 2 leads to a value of 0.083 for the ratio of the finite rate of growth to the rate of coke formation corresponding to the instantaneously reached intermediate size, $r_p^\circ/C_t M_{CI} R_s^\circ$. The corresponding contributions to the coke content in the pores which cannot be blocked follow from the ratio of the second to the first term in (21). An experimental run lasted 1 to 2 h, well beyond the industrial on-stream time. At that time both contributions become of the same order of magnitude.

The relative importance of these two contributions as well as the molecular mass of the coke molecules both depend on time and process conditions. This also holds for the related properties. At the end of the experimental run under the conditions dealt with in Fig. 2, up to 14.8% of the catalyst surface area is inaccessible as a result of pore blockage either by the instantaneously grown coke alone or by coke further grown at a finite rate. This corresponds to a pore diameter of 3.47 nm. The coke content in the larger pores results for 93.3% from growth of the coke at a finite rate.

Finally it should be noted that the parameters occurring in the rate expression for fractional site coverage [Eq. (8)] are identical in the two models considered. Most of the corresponding estimates in Tables 1 and 2 are not significantly different at the 95% confidence level. This should be expected since the only difference between the two models resides in the growth mechanism.

As shown by Eqs. (4)–(6), there is no a priori reason why r_p°/R_s° should be independent of the process conditions. Several expressions for the rate of coke formation due to growth at a finite rate different from Eq. (8) for the rate of fractional site coverage were tested. They did not give rise to an improved significance of the global regression.

3. Influence of Coke Deposition on the Activity for Butene Dehydrogenation

Dumez and Froment (15) obtained a few sets of data on the deactivation function for dehydrogenation, ϕ_A, as a function of coke content by on-line coupling of a gas chromatograph to the electrobalance reactor setup. The activity of the catalyst for dehydrogenation decreased to values below one-fifth of its original activity, as illustrated in Fig. 3. It follows from the preceding section that this cannot be caused by blockage of pores alone. Hence, it is reasonable to assume that the active sites for dehydrogenation are the same as those for coke formation.

Dumez and Froment (15) also carried out a kinetic analysis of the dehydrogenation reaction on the uncoked catalyst. Out of 15 a priori possible rate equations, an equation corresponding to a mechanism with a rate-determining step involving two active sites was selected on the basis of statistical criteria. The F value for the global regression of the dehydrogenation rate data with the rate equation selected by Dumez and Froment amounts to 973. A regression with the rate equation not considered by Dumez and Froment (15),

$$r_A^\circ = \frac{A^\circ \exp(-E/RT)(p_A - p_D p_H/K)}{1 + K_A p_A + K_D p_D + K_H p_H}, \quad (23)$$

yields an F value of 1041. Since Eq. (23) corresponds to a mechanism involving a single site in the rate-determining step, the expressions for ϕ_A derived by Beeckman and Froment (1, 2) are applicable.

These expressions take the coking kinetics into account explicitly. Again instantaneous growth followed by growth at a finite rate is considered. The deactivation function for the dehydrogenation, averaged over the pores with diameter D, is given by

$$\hat{\varphi}_A(D,t)$$

$$= \left\{1 - \left[\frac{(\sigma(D)/\nu)(1 - \exp(-R_s^\circ t))}{1 + (\sigma(D)/\nu)(1 - \exp(-R_s^\circ t))}\right]^2\right\}$$

$$\exp(-R_s^\circ t) \quad (24)$$

for the small pores which can be blocked immediately after coverage.

For the pores too large to be blocked, the expression for the deactivation function is simplified to

$$\hat{\varphi}_A(D,t) = \exp(-R_s^\circ t). \quad (25)$$

For pores with an intermediate diameter the deactivation function is given by

$$\hat{\varphi}_A(D,t)$$

$$= \left\{1 - \left[\frac{(\sigma(D)/\nu)}{1 + (\sigma(D)/\nu)}\frac{(1 - \exp(-R_s^\circ(t - t_b(D))))}{(1 - \exp(-R_s^\circ(t - t_b(D))))}\right]^2\right\}$$

$$\exp(-R_s^\circ t) \quad (26)$$

as soon as growth can cause blockage. The global deactivation function for the dehydrogenation, ϕ_A, is obtained from

$$\Phi_A(t) = \int_0^\infty g^S(D)\hat{\varphi}_A(t) \, dD. \quad (27)$$

Elimination of the process time from Eqs. (22) and (27) and use of the parameter values listed in Table 2 and obtained from the coking curves only lead to the calculated ϕ_A versus C_C curve. An example of such a curve for typical deactivation conditions is shown in Fig. 3. The sharp initial decrease of the deactivation function corresponds to the fraction of the surface area which is rendered inaccessible by blockage of the smallest pores. The agreement with the experimental data is more than satisfactory. This is a striking result, since no curve fitting was involved.

This prediction of the effect of coke on the rate of dehydrogenation shows the adequacy of the model. Ideally, however, the coking kinetics should be determined simultaneously with the effect of coke on the main reaction, as outlined in Fig. 4. Obtaining expressions for R_s° and/or r_p° from observations both on the deactivation of the main reaction and on the coke content is obviously to be preferred to obtaining it from either the main reaction or the coke content only. A multiresponse nonlinear regression will avoid producing different estimates for the parameters in R_s° and/or r_p° from both types of information. The objective function, F, contains weight factors w_1 and w_2, while l_1 and l_2 are the numbers of data points on r_A and C_C, respectively. The symbols $\hat{r}_{Ai}$ and $\hat{C}_{Ci}$ represent calculated values for r_{Ai} and C_{Ci} based on the kinetic models to be tested. The number of data points l_1 on the dehydrogenation of butene was too small to allow a data analysis along these lines.

CONCLUSIONS

Catalyst deactivation by coke deposition in butene dehydrogenation on Cr_2O_3/Al_2O_3 can be adequately described in terms of ac-
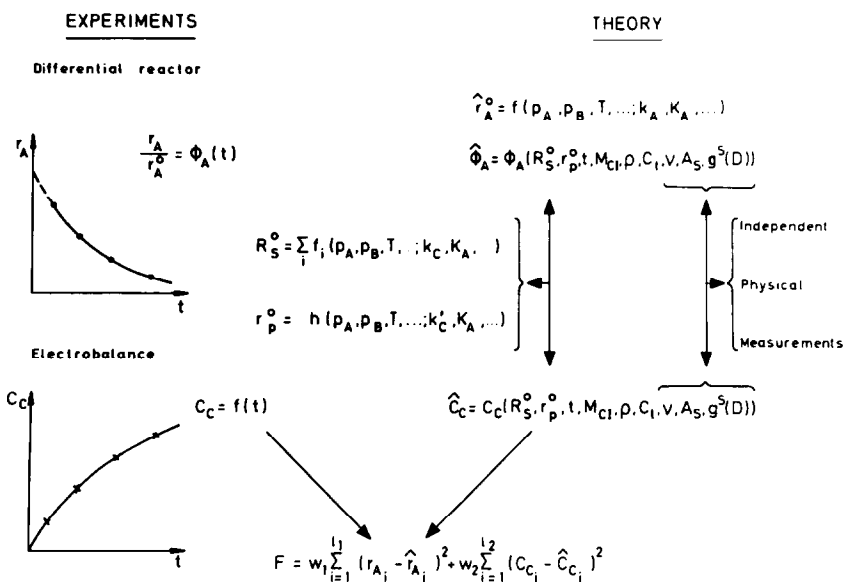
FIG. 4. General approach for a kinetic analysis of main and coking reaction (3).

tive site coverage and pore blockage. The growth of the coke occurs at a rate which is of the same order of magnitude as the rate of fractional site coverage. For typical industrial run lengths only 15% of the catalyst surface area becomes inaccessible as a result of pore blockage. Most of this blockage occurs during the first seconds of operation and is caused by only 0.01% of the total amount of coke which can be deposited on the catalyst. Both coke formation and dehydrogenation are catalyzed by the same type of active sites.

The approach followed in this work can be applied to other catalysts as well and hence can contribute to a better understanding of the mechanisms underlying their deactivation. This understanding should contribute to a more accurate "tailoring" of new catalysts.

APPENDIX: NOMENCLATURE

A Butene

A° Preexponential factor (1/bar · h)

A_S Specific catalyst surface area (m^2/kg cat)

C_C Coke content of the catalyst (kg coke/kg cat)

C_t Total concentration of sites (kmol sites/kg cat)

$\hat{C}_C(D,t)$ Average coke content in pores of diameter D (kg coke/kg cat)

D Butadiene

D Diameter of a pore (m)

D_C Diameter of a coke molecule (m)

E Apparent activation energy (kJ/kmol)

F Ratio of the mean regression sum of squares to the mean residual sum of squares

$g^S(D)\ dD$ Fractional surface area of pores with diameter between D and $D + dD$

H Hydrogen

k_C Rate coefficient for a single site coking reaction (kg coke/kmol sites h)

K Equilibrium coefficient for dehydrogenation (bar)

K_A Adsorption coefficient of component A (1/bar)

L Length of a pore (m)

M_C Molecular mass of coke (kg coke/kmol coke)

M_{CI} Molecular mass instantaneously reached after coke precursor formation (kg coke/kmol coke)

M_C^* Molecular mass of a coke molecule on a site covered at time t^* (kg coke/kmol coke)

N_A Avogadro number (1/kmol)

p_A partial pressure of component A (bar)

P accessibility function, i.e., the probability of a site being accessible

r specific rate of reaction (kmol/kg cat · h)

r° specific rate of reaction in the absence of coke (kmol/kg cat · h)

r_p° rate of growth of coke (kg coke/kg cat · h)

$r_{s,i}^\circ$ Rate of fractional site coverage according to reaction path i (1/h)

R Ideal gas constant (kJ/kmol K)

R_s° Total rate of fractional site coverage (1/h)

S Probability that an accessible site is not covered

t Time (h)

t^* Time at which a site is covered (h)

t_b Time required for a precursor to grown into a coke molecule with the size of the pore (h)

T Temperature (K)

$V(D)$ Molar volume of coke which blocks a pore with diameter D (m³/kmol coke)

V_C^* Volume of a coke molecule on a site covered at time t^* (m³)

Greek Symbols

γ Fractional surface area of the pores which can be blocked

$\lambda(L)\ dL$ Probability that a pore has a length between L and $L + dL$

$\nu\ dx$ Probability that a pore branches in an interval dx

ρ Density of coke and coke precursor (kg coke/m³)

$\sigma(D)\ dx$ Probability that a site is located in an interval dx in a pore of diameter D

$\hat{\varphi}_A(D,t)$ Global deactivation function for the dehydrogenation in pores of diameter D

ϕ Deactivation function for a reaction

ϕ_A Deactivation function for dehydrogenation

ϕ_C Deactivation function for coking

REFERENCES

1. Beeckman, J. W., and Froment, G. F., *Ind. Eng. Fundam.* **18**, 245 (1979).
2. Beeckman, J. W., and Froment, G. F., *Chem. Eng. Sci.* **35**, 805 (1980).
3. Froment, G. F., in "Progress in Catalyst Deactivation" (J. L. Figueiredo, Ed.), NATO Advanced Study Institutes Series, E54, p. 103. Nijhoff, The Hague, 1982.
4. Wilson, R. J., and Beineke, L. W., in "Applications of Graph Theory" (R. J. Wilson and L. W. Beineke, Eds.), p. 1. Academic Press, New York/London, 1979.
5. Fisher, M. E., and Essam, J. W., *J. Math. Phys.* **2**, 609 (1961).
6. Shante, V. K. S., and Kirkpatrick, S., *Adv. Phys.* **20**, 325 (1971).
7. Voorhies, A., *Ind. Eng. Chem.* **37**, 318 (1945).
8. Corma, A., and Wojciechowski, B. W., *Catal. Rev. Sci. Eng.* **24**, 1 (1982).
9. Nace, D. M., Voltz, S. E., and Weekman, V. M., *Ind. Eng. Chem. Process Des. Dev.* **10**, 530 (1971).
10. Mahoney, J. A., *J. Catal.* **32**, 247 (1974).
11. Corella., J., Asua, J. M., and Bilbao, J., *Chem. Eng. Sci.* **35**, 1447 (1980).
12. Absil, R. P. L., Butt, J. B., and Dranoff, J. S., *J. Catal.* **85**, 415 (1984).
13. Pacheco, M. A., and Petersen, E. E., *J. Catal.* **86**, 75 (1984).
14. Wheeler, A., *Adv. Catal.* **3**, 249 (1951).
15. Dumez, F., and Froment, G. F., *Ind. Eng. Chem. Process Des. Dev.* **15**, 291 (1976).

16. Levinter, M. E., Panchenkov, G. M., and Tana-
tarov, M. A., *Int. Chem. Eng.* **7**, 23 (1967).

17. Abbott, H. W., *in* "Encyclopedia of Chemical
Technology" (R. E. Kirk and D. F. Othmer,
Eds.), p. 1. Wiley–Interscience, New York, 1949.

18. Burwell, R. L., Haller, G. L., Taylor, K. C., and
Read, J. F., *Adv. Catal.* **20**, 1 (1969).

19. Weller, S., and Voltz, S. E., *J. Amer. Chem. Soc.*
76, 4695 (1954).

20. Draper, N. R., and Smith, H., "Applied Regres-
sion Analysis." Wiley, New York, 1966.